frontiers | Frontiers in Earth Science

TYPE Original Research
PUBLISHED 03 June 2024
DOI 10.3389/feart.2024.1402474



OPEN ACCESS

EDITED BY
Chenyang Zhang,
Hong Kong Polytechnic University, Hong Kong SAR, China

REVIEWED BY
Jinge Zhang,
Nagasaki University, Japan
Tianqi Jiang,
Kyushu University, Japan
Longfei Zhang,
Southwest Jiaotong University, China

*CORRESPONDENCE
Jiabing Zhang,
jxsi342@163.com

RECEIVED 17 March 2024
ACCEPTED 09 May 2024
PUBLISHED 03 June 2024

CITATION
Xu P, Xing X, Jin C, Wang R, Zhang J and Zhang X (2024), Study on pile-soil contact effect of anti-sliding piles in swelling soil landslides.
*Front. Earth Sci.* 12:1402474.
doi: 10.3389/feart.2024.1402474



# Study on pile-soil contact effect of anti-sliding piles in swelling soil landslides

Peng Xu[1], Xiansen Xing[2], Chengcai Jin[1], Ruiying Wang[3], Jiabing Zhang[4]* and Xiaohu Zhang[5]

[1]Liaoning Non-Ferrous Geological Exploration and Research Institute Co., Ltd., Shenyang, China, [2]School of Earth Sciences and Engineering, Hohai University, Nanjing, China, [3]Shenyang Geotechnical Investigation & Surveying Research Institute Co., Ltd., Shenyang, China, [4]College of Construction Engineering, Jilin University, Changchun, China, [5]School of Civil Engineering, Guizhou University of Engineering Science, Bijie, China

In recent years, it is not uncommon for swelling soil landslides to occur again after treatment, which has seriously affected the safe operation of highways and railways. The degree of consolidation and cementation of swelling soil is poor, and its fractures are developed and it has a certain expansibility. Under the action of expansion force, its shear strength is obviously reduced. Thus, anti-slide pile support is used to control swelling soil landslides in this study. Based on the geological conditions and genetic mechanism of swelling soil landslide, a three-dimensional geological model with a width of 40 m is established to simulate the interaction mechanism and influencing factors between soil and pile in the process of anti-slip pile support. The results show that the larger the cohesion and internal friction angle, the stronger the soil arch effect, but the sensitivity is higher when the value is small. Therefore, attention should be paid to the weakening effect of soil arch effect in soil with low shear strength. The larger the pile spacing, the less obvious the soil arch effect. The swelling force also has a great influence on the soil arch effect from scratch. With the increase of the expansive force, the soil arch effect is weakened and completely disappears. Therefore, the adverse effects of expansive force should be considered, when designing anti-slide piles in swelling soil areas.

KEYWORDS

**swelling soil landslide, anti-slide piles, soil arch effect, FLAC 3D, slope**

## 1 Introduction

Under the influence of disturbance factors such as rainfall and excavation, swelling soil are easy to cause engineering disasters such as slope instability due to their unique engineering characteristics. It has always attracted much attention in geotechnical engineering (Zhu et al., 2020; Fang et al., 2023; Li et al., 2023; Zhang et al., 2024). As a retaining and anti-slide structure with simple construction and good anti-slide effect, the anti-slide pile is widely used in landslide protection and treatment (Wang et al., 2022; Wang et al., 2023). When the slope is unstable, the force on the anti-slide pile is very complicated. With the continuous study of anti-slide piles by scholars for years, it is found that there is a kind of arching effect between pile and soil. This arching effect can deflect the stress and transfer the sliding thrust of the landslide to the anti-slide pile (Li et al., 2021; Zhang et al., 2021). Due to the poor consolidation and cementation of swelling soil, its physical

properties are greatly affected by changes in environmental factors. It is prone to repeated expansion and contraction, so the internal fractures continue to develop and increase, and the strength of soil is low (Xu, 2020; Tian et al., 2021), which makes the interaction mechanism of this pile-soil effect more complicated. To improve the supporting effect of anti-slide piles in swelling soil, the mechanism and influencing factors of the soil arch effect should be studied fundamentally.

The key to studying the pile-soil effect is the interaction between the pile and the soil around the pile. The pile-soil effect is affected by the geometric parameters and physical parameters of the pile and the soil, including the layout of the pile in the soil and the number of layouts (Ren et al., 2022; Wang et al., 2024). Owing to the difficulty of visualization of the pile-soil effect, it is difficult to carry out indoor tests. Many researchers take the numerical simulation method as the main means to analyze the pile-soil effect. The soil arch effect is divided into three evolution stages: formation stage, development stage, and destruction stage (Sun et al., 2019). Based on the mechanical calculation model of inclined pile soil arch, the influence of sliding force, pile width, cohesive force, and internal friction angle of soil on the arching condition and design pile spacing was studied by Liu et al. (2021) Pile-soil stress ratio is an important parameter for the calculation of bearing capacity and settlement of pile-soil composite foundation, which is affected by the consolidation and settlement state of the foundation and has obvious time-varying characteristics. Based on the Terzarghi model, the quantitative variation of pile-soil stress with various design parameters is systematically analyzed (Huang et al., 2020). The research showed that increasing the filling load has a significant weakening effect on the soil arch effect, and the pile-soil stress ratio decreases with the increase of pile spacing. Wang (2022) analyzed the spatial distribution law of the soil arch effect by finite element numerical simulation software. The results showed that when the pile spacing reaches four times the pile width, the soil load sharing ratio increases significantly and tends not to change with the further increase of pile spacing. Based on the indoor model test, Deng et al. (2022) found that the distribution of pile-soil stress in the cross-sectional direction of the subgrade is greater than its longitudinal extension direction, which is related to the trapezoidal cross-section design of the subgrade. Based on the finite difference numerical simulation software, Hu (2022) found that the soil arch effect can be significantly enhanced when the internal friction angle and cohesion of soil increase within a certain range. By analyzing the pile-soil interaction through the indoor model test and finite element analysis method, Deng et al. (2024) found that the bearing capacity of rigid piles and semi-rigid piles is mainly shared by side friction. Han (2021) analyzed the pile-soil effect of pile group foundations under horizontal load by finite element software. The study showed that the increase in pile number makes the stress of soil between piles overlap, the horizontal bearing capacity of the pile group increases, and the efficiency of the pile group decreases. Under the action of horizontal static load, the internal force of the pile body is mainly concentrated in the upper half of the soil layer.

The Swelling soil have strong water absorption. After the drying-wetting cycle, its physical properties will change greatly, and it has obvious expansion and contraction properties (Fang et al., 2021; Dai et al., 2024). The safety factor of expansive soil slope decreases rapidly and then slowly with the increase of drying-wetting cycle times, and the effect of expansive force will further aggravate the risk of instability and failure of expansive soil slope (Yang et al., 2022; Zhang et al., 2022). Therefore, it is necessary to analyze the influence of expansive force on the soil arch effect. The expansive force will change the stress mode of the pile-soil so that the soil arch at the end of the pile is transformed into the friction soil arch at the side of the pile (Ding et al., 2022). The "wet expansion and dry contraction" effect of expansive soil with smaller initial water content is significant. When it absorbs water and expands, it will produce a very large expansion rate and expansive force, resulting in instability and failure of surrounding rock slopes (Zhang et al., 2018). Zhang et al. (2020) revealed the changing law of the lateral expansive force of expansive soil under the influence of vertical expansion and lateral expansion and established the corresponding relationship expression. Through the expansion pressure test of expansive soil, Tan et al. (2024) found that the vertical expansive force is higher than the lateral expansive force, and the reduction of the lateral expansive force can significantly increase the sliding stability coefficient of the retaining wall.

Through reading and analyzing the relevant literature at home and abroad, it is found that there is no unified and clear theoretical understanding of the influencing factors of the soil arch effect, the load transfer law, and its application in engineering governance. The scientific problems such as the function mode of pile-soil effect in pile group and the interaction mechanism between upper load and pile-soil effect are worthy of further discussion (Hu et al., 2021; Liu et al., 2023). In addition, the statics study of pile-soil effect is helpful to the dynamic response study of pile-soil effect (Xu et al., 2021). Therefore, to further study the influence of the pile-soil effect of anti-slide piles on engineering construction, this paper constructs a three-dimensional geological model of an anti-slide pile in Xinyan landslide based on the FLAC3D numerical simulation method. The pile-soil interaction was analyzed from many aspects, including the influence of the pile-soil contact interface, the shear strength parameters of soil, the pile spacing and the expansibility of swelling soil landslides on the shape of soil arch effect, and the pile-soil bearing ratio, which provides data support and scientific reference for engineering construction.

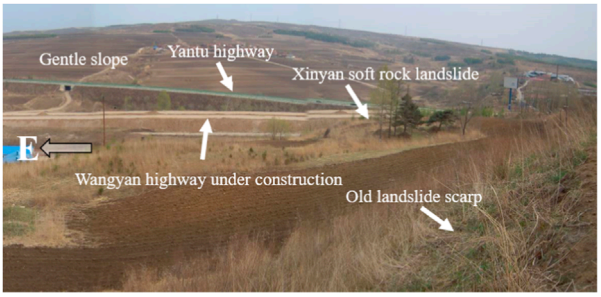


FIGURE 1
Topography of Xinyan soft rock landslide.

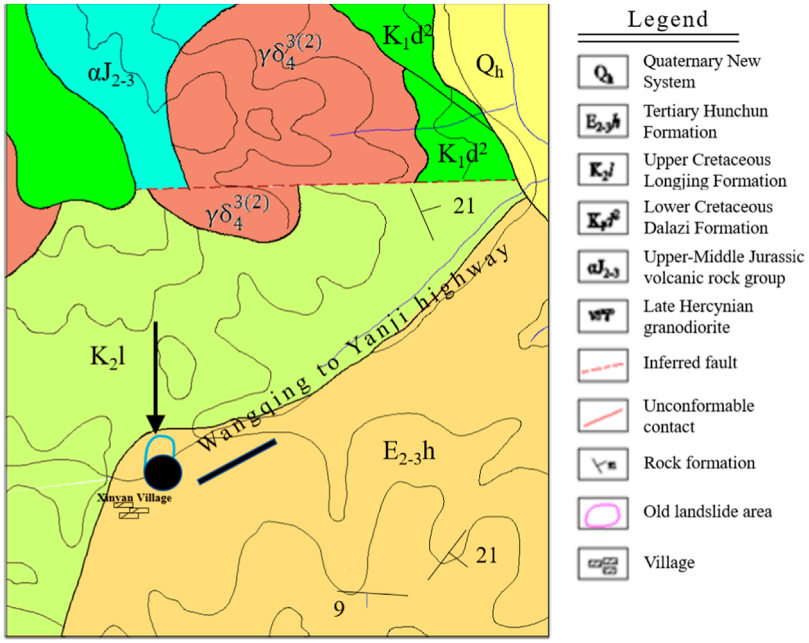


FIGURE 2
Plane graph of landslide.

## 2 Overview of xinyan landslide

The swelling soil landslide is located in Xinyan village, the northern suburb of Yanji city, Jilin province, as shown in Figure 1. The area is a low hilly area with relatively developed vegetation and undulating topography, transitioning to low mountains in the north. The slope is a step-like slope with a gentle inclination to SE. The slope of the ground is generally 10°–35°, and the bottom of the slope is slightly steep. The relative height difference is more than 10 m, and the terrain is relatively open. There are small shallow gullies developed near the landslide site. As shown in Figure 2, the lithology is mainly Cenozoic Tertiary Hunchun Formation (E2-3 h), which is composed of grayish-yellow mudstone, fine sandstone, and gravel-bearing coarse sandstone. The occurrence of rock strata is 88°∠15° and the rock has a high degree of weathering and low strength.

The classification of underground water is mainly loose rock pore water. The nearly horizontal sand layers, sandstone lenses, sandstone interlayers, and joint fissures developed in rock layers accelerate the runoff and seepage of groundwater, which saturates and softens the soil. The soil in the slope is soft, and the mineral components in the mudstone interlayer of the Quaternary strata and the Tertiary Hunchun Formation are mainly montmorillonite and illite (content is 16%–53%), which are easy to absorb water and expand and make slope creep imbalance.

The Xinyan swelling soil landslide is mainly caused by the new fill section. The total area of the plane is about $1.7 \times 10^4$ m$^2$, the height of the landslide is about 15 m, the thickness of the landslide body is about 3–5 m in the front part, 5–15 m in the middle part, and 3–5 m in the back part, and the average thickness of the landslide body is about 8 m, and the total volume is about $13.6 \times 10^4$ m$^3$. As shown in Figure 3, the landslide material is mainly composed of filling soil, silty clay, and fully weathered mudstone sandstone.

The leading edge of the landslide is located near the Xiaohegou on the south side of the Wangyan highway. The damage of the leading edge can be clearly seen at the scene of the exploration area from Figure 4. Through the investigation, it is found that the number of tensile fractures and bulging fractures on the landslide body is significantly increased compared with the previous field investigation. There are obvious stepped tensile fractures on the south side of the high-grade highway pavement and the slope. The trend is basically parallel, mostly in the northeast direction, which is perpendicular to the sliding direction of the landslide. The depth is between 0.1 m and 0.6 m, the length is different, and the width is between 0.1 m and 0.95 m. The fracture size is obviously larger than that seen in the previous investigation.

## 3 Analysis of pile-soil effect of anti-slide pile

The soil arch effect is a complex three-dimensional stress transfer mechanism. The displacement direction of the slope soil may not be in the horizontal plane, the pile body has a certain lateral displacement in the slope, and the pile bottom is not completely fixed.

### 3.1 Model establishment and parameter selection

As an intuitive and effective method, numerical simulation has been widely used in the study of the soil arch effect between pile and

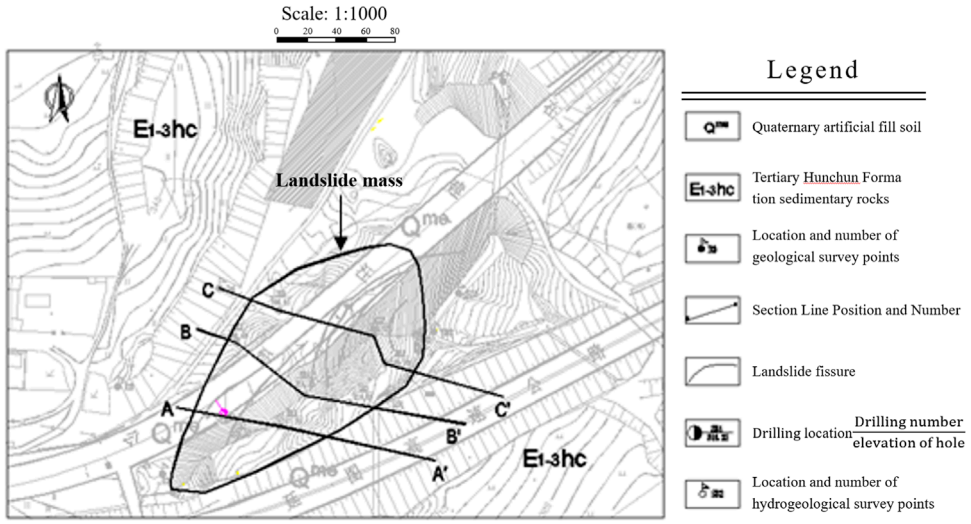


FIGURE 3
Regional geological map of landslide area.


FIGURE 4
Failure phenomenon of the leading edge of landslide.

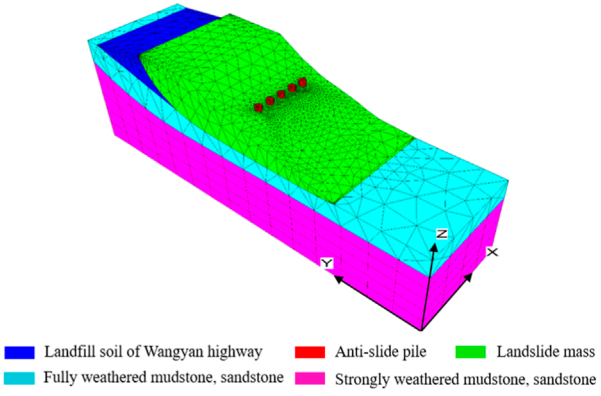


FIGURE 6
Schematic diagram of the three-dimensional model and mesh generation.

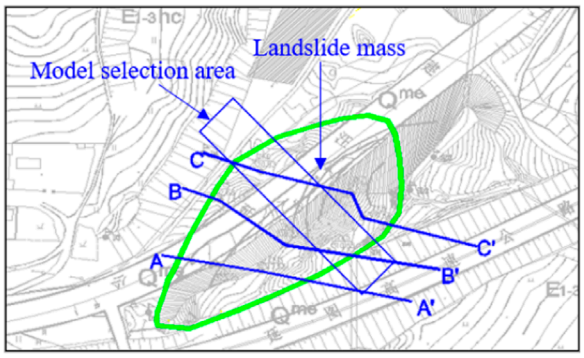


FIGURE 5
Schematic diagram of model area.

soil. In this paper, the pile-soil effect of the anti-slide pile in Xinyan landslide is analyzed by the three-dimensional model, so that the simulation conditions are closer to the engineering practice. In this model, the width of 40 m in the middle of the landslide is selected as the research object, as shown in Figure 5. To prevent the boundary effect from affecting the study area, the model size should be larger than the study area, and the size is set to 145 m long and 46 m high.

Because of the powerful pre-processing function of ANSYS, the construction of the geometric model and the division of the grid are completed in ANSYS. Horizontal constraints are imposed on both sides ($x$ direction), front and back ($y$ direction) of the model, and vertical constraints are imposed on the bottom ($z$ direction) of the model. The constructed model and coordinate direction are shown in Figure 6. The Elastic model is used for the anti-slide pile, the Mohr-Coulomb model is used for landslide mass, and the "interface element" without thickness is used for the pile-soil

TABLE 1 Statistics of model parameters.

| Name | Density (kg/m3) | Poisson ratio | Compressic modulus (MPa) | Bulk modulus (MPa) | Shear modulus (MPa) | Internal friction angle (°) | Cohesion (MPa) | Tensile strength (MPa) |
|---|---|---|---|---|---|---|---|---|
| Anti-slide pile | 2,500 | 0.15 | 25000 | 11904 | 10869 | | | |
| Landfill soil of Yantu highway | 1890 | 0.34 | 40 | 39.22 | 15.04 | 20.00 | 20.00 | 0.03 |
| Landslide mass | 1890 | 0.35 | 30 | 33.33 | 11.11 | 7.00 | 15.00 | 0.02 |
| Fully weathered mudstone, sandstone | 1950 | 0.32 | 50 | 46.30 | 18.94 | 17.00 | 25.00 | 0.03 |
| Strongly weathered mudstone, sandstone | 2000 | 0.30 | 2000 | 1,667.00 | 769.23 | 25.00 | 50.00 | 0.03 |

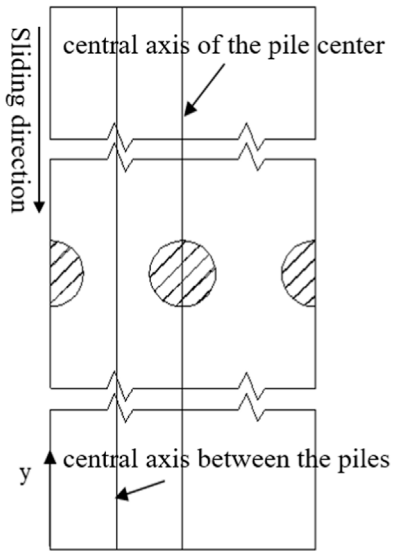


FIGURE 7
Schematic diagram of section.

interface. More detailed element division is carried out in the pile and its surrounding key research areas. This model is divided into 48814 elements and 10201 nodes. The specific parameters of the model are shown in Table 1.

## 3.2 Study on pile-soil effect of anti-slide pile

To find out the effect of pile-soil interaction, the construction model is analyzed according to the design results of the B-B section. The diameter of the anti-slide pile is 2.5 m, the center distance of the pile is 5 m, the length of the pile is 14 m, and the length of the embedded section is 5 m. In the following analysis, the central axis of the pile center and the central axis between the piles will be used. The specific position is shown in Figure 7, and the sliding direction of the landslide is negative *y* direction. The program of the maximum and minimum principal stress of the section at the central axis between the piles are shown in Figure 8. It can be seen that the maximum principal stress in front of the pile appears obvious tensile stress zone, while the minimum principal stress after the pile appears obvious stress concentration.

As shown in Figure 9-1, a part of the pile body in front of the pile is subjected to tensile failure, which is consistent with the stress distribution of the pile. As shown in Figure 9-2, it can be seen that the maximum principal stress on the pile is basically in the vertical direction, and the minimum principal stress is basically in the horizontal direction. This phenomenon is caused by the soil arch effect. In the process of pile-soil interaction, the formation of soil arch effect is the process of stress transfer, which means that the stress of soil is transferred to the pile. These stresses act on the back of the pile in a nearly orthogonal direction, resulting in the phenomenon that the minimum principal stress is concentrated behind the pile. In the meantime, due to the thrust behind the pile and the blocking effect of the soil in front of the pile, a tensile stress zone is generated in a certain range in front of the pile. It can be seen that the anti-slide pile is not a simple stress state of a single pile, and the pile-soil interaction is a complicated stress state. The influence of the soil arch effect should be fully considered in the design of anti-slide pile support and pile strength.

Figure 10 shows the distribution of σy at different depths of the pile top perpendicular to the *z*-axis. With the increase of depth, the soil arch effect in front of the pile decreases continuously, and the soil arch effect behind the pile increases continuously, while the soil arch effect disappears when the depth is more than 9 m. The depth of the sliding surface at the location of the anti-slide pile is about 11.5 m, and the soil arch behind the pile is the most obvious in the range of 5–9 m depth, and the soil arch at a depth of 11 m disappears. It can be seen that the soil arch effect begins to form in the middle of the sliding body, which is most significant in the middle and lower part

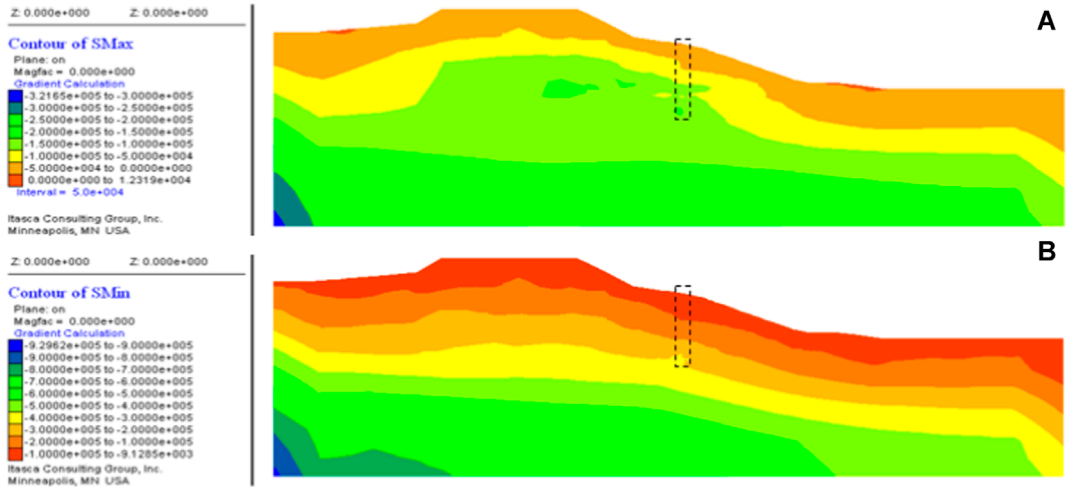


FIGURE 8
Stress nephogram of the section between piles: **(A)** maximum principal stress; **(B)** minimum principal stress.

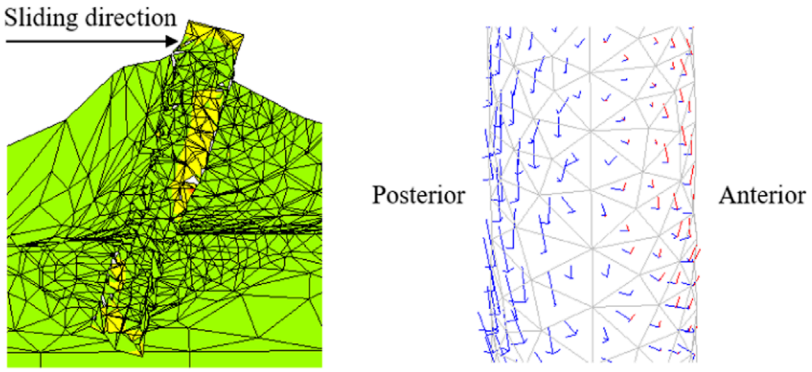


FIGURE 9
Deformation effect of pile body. Figure 9-2 Schematic diagram of principal stress of pile body.

of the sliding body, and gradually weakens and disappears near the sliding surface.

Under the action of landslide thrust, the soil between piles tends to extrude forward. It can be seen from the figure that the existence of stress arch is obvious, and the shape of stress arch changes significantly with the change of depth. Due to the blocking effect of the anti-slide pile, the stress of the soil in front of the pile is very small. Thus, the stress deflection occurs, and the soil arch is generated on the passive side of the pile. With the increase in depth, the displacement of the pile decreases, and the relative displacement between the pile and soil increases. The frictional resistance and cohesive force between the pile and the soil begin to play a role in preventing the soil from sliding through the pile. As a result, the relative displacement of the soil in front of the pile and behind the pile is caused, and the "wedge tightening" effect of the soil behind the pile is strengthened, and the soil arch effect is produced. With the increase of the soil arch effect after the pile, the stress in the soil is gradually transferred to the pile, and the soil arching caused by the sliding of the soil in front of the pile is gradually weakened.

It can be seen from Figure 10 that the soil arch effect is the most significant when the depth is 7–9 m. This is in the same depth as the pile stress concentration and tensile stress zone in Figure 8, which can further verify that the formation of the tensile stress zone is directly related to the generation of soil arch. When the depth is 11 m, the soil arch effect is very weak. This is because the displacement of the soil at this depth is very small, and the relative motion of the pile and soil is not obvious.

The cross-section with a depth of 7 m was taken out, and the distance nephogram of the section in the *y* direction is shown in Figure 11. It can be seen that the displacement nephogram behind the pile has an obvious arch shape. The displacement on the central axis between piles is slightly smaller than the displacement of the soil behind the piles on both sides. It shows that in the formation process of the soil arch effect, with the completion of stress deflection, the soil behind the pile also forms an arch structure which is conducive to resisting landslide thrust in spatial form.

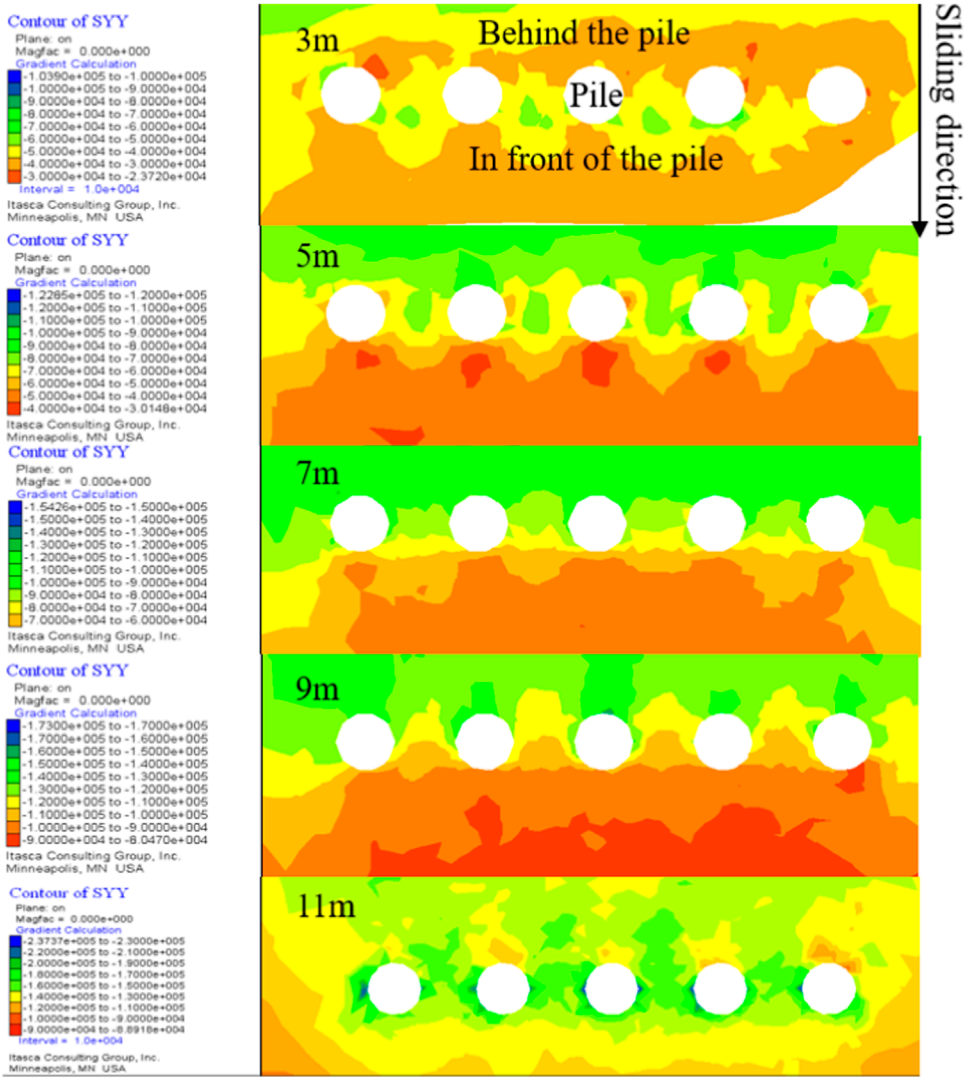


FIGURE 10
The distribution of σy in different depths.

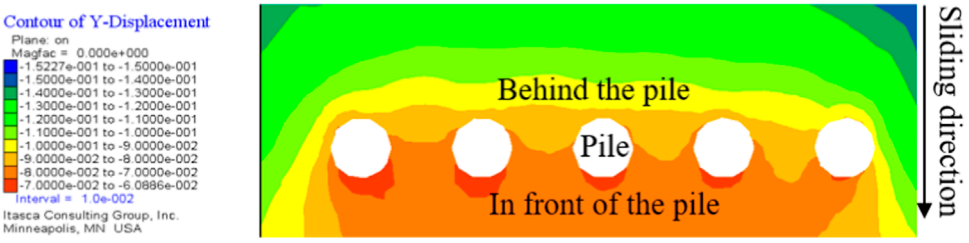


FIGURE 11
The distance nephogram of section in *y* direction.

In order to analyze the formation process of soil arching, the σy of each point on the central axis between piles is drawn into a curve as shown in Figure 12. The ordinate in the diagram is the distance from the anti-slide pile. The positive value indicates the rear of the pile, while the negative value indicates the front of the pile. It can be seen that the stress curve has an obvious change trend at different positions. Under the action of sliding thrust, the σy of each point on the central axis is roughly divided into four stages:

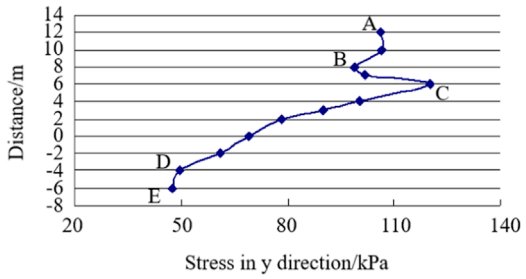


FIGURE 12
The σy curve of each point on the central axis between piles.

A-B: The soil is far away from the pile, not affected by the anti-slide pile, and stress has a small range of changes under the action of landslide thrust. B-C: The anti-slip piles start to work. Stress increases at the formation of the soil arch, reaching a maximum at the top of the arch. C-D: The soil arch effect is obvious, where σy begins to decrease sharply, and the soil stress begins to transfer to the pile body. The rate of decrease becomes smaller at the center point between piles. At this time, the soil arch effect begins to weaken and gradually disappears. D-E: Farther away in front of the pile, the soil arch effect disappears completely and the stresses change slowly under the sliding thrust.

As a quantitative index, load sharing ratio plays an important role in soil arching analysis. During the anti-slide process of the pile, only part of the landslide thrust behind the pile can be transmitted to the front of the pile. The soil and the pile bear part of the load respectively, and the proportion of the total load borne by the pile and the soil is defined as the pile-soil load-sharing ratio; Considering the feasibility of the three-dimensional model calculation, the cross-section of $z$ = 314 m is taken as the research object when calculating the load. A profile line parallel to the $x$ direction is made at 0.5 m in front of the pile, and σy on the profile line between two adjacent piles is calculated and plotted as a curve. The area enclosed by the curve is the load transmitted to the front of the pile. A profile line parallel to the $x$ direction is made outside the influence range of the soil arch effect behind the pile, and the load at this position without an anti-slide pile is calculated as a total load of landslide thrust. The ratio of the difference between the two loads and the landslide thrust load is the load-sharing ratio of the pile. The distribution of σy behind and in front of the pile is shown in Figure 13.

Figure 13-1 The σy curve of section at 0.5 m in front of the pile Figure 13-2 The σy curve of section at 0.5 m behind the pile.

From Figure 13-2, it can be calculated that the thrust of the landslide after the pile is 700 kN/m. Figure 13-1 shows that the residual sliding force in front of the pile is 225 kN/m. Accordingly, it can be calculated that the load-sharing ratio of the pile is 68%. This research can better form the soil arch effect and give full play to the interaction between pile and soil. The load-sharing ratio of the pile is 68%, which shows that the anti-slip pile bears most of the downward thrust and can provide a good anti-slip effect.

## 3.3 Analysis of the influence of cohesion on soil arching

Soil cohesion has an important effect on landslide stability. The formation of soil arch is a kind of "'wedge tightening" effect between soil particles, so the cohesion should have a certain influence on the soil arch effect. Four different cohesions of C = 5 kPa, 17 kPa, 25 kPa, and 35 kPa are set for calculation, as shown in Figure 14.

It can be seen from Figure 14 that there is no soil arch formation when C = 5 kPa and the stress value is large. It can be seen from Figure 15 that due to the small cohesion of the slope, a large number of shear failure areas appear in the slope, and the slope has been destabilized. The soil arch effect is most obvious when C = 17 kPa and the arch height decreases gradually when C = 25 kPa and 35 kPa. This is due to the increase of cohesion, the slope stability is enhanced, and the relative displacement of pile and soil is reduced. With the increase of cohesion, the ring-shaped small stress zone gradually appears in front of the pile, and the stress value is getting smaller, indicating that the anti-sliding effect is enhanced. The shape of the soil arch on the passive side of the pile gradually transitions from a circular arc to a similar isosceles triangle. The stress concentration area on the anti-slide pile is gradually transferred from the back of the pile to the side of the pile. It illustrates that the soil arching behind piles plays a major role in the slope with a small C value, while the soil arching between piles plays a major role in the slope with a high C value.

The σy curve on the central axis between piles is shown in Figure 16. Since the slope has been destabilized when C = 5 kPa, the calculation does not converge, so the results when C = 5 kPa are not included in the statistics. It can be seen from the figure that the inflection points of the three cases begin to appear from 7 m behind the pile, and the soil arch effect starts to work. The soil arch effect starts to weaken and disappears when the pile centerline is reached. According to the variation range of the curve, it can be found that the soil arch effect is the most obvious when C = 17 kPa. The lower the cohesion, the greater the sliding thrust acting on the pile. The stress before the pile changes little in the three cases, which means that the soil arch effect is adequately effective and has provided a better anti-slip effect when C = 17 kPa and it is uninfluential to improve cohesion for anti-slide effect.

## 3.4 Analysis of the influence of internal friction angle on soil arching

Keeping the other parameters of the model unchanged, the influence of the internal friction angle on the soil arch effect is analyzed by changing the internal friction angle. Four cases of φ=3°, 10°, 17° and 25° are set for calculation; As shown in Figure 17, the influence of internal friction angle on the soil arch effect is roughly the same as that of cohesion. There is almost no soil arch effect because the angle of internal friction is too small for the "wedge tightening" effect between the soil particles when φ=3°. The soil arch effect is most obvious when φ=10° φ=17° and 25°, the arch height of the soil arch decreases gradually, which is also due to the increase of internal friction angle, the enhancement of slope stability and the decrease of relative displacement between pile and soil. As the internal friction angle increases, the stress value in front of the pile

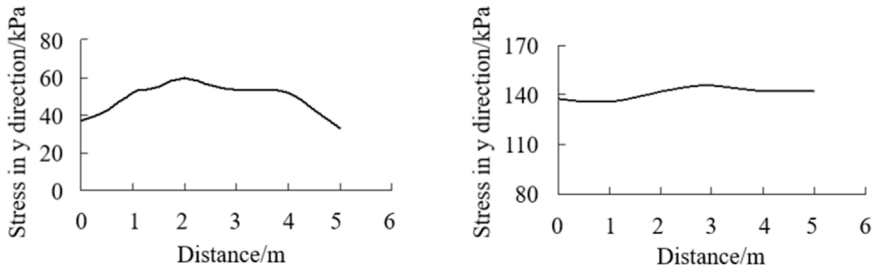


FIGURE 13
Theσy curve of section at 0.5 min front of the pile. Figure 13-2 Theσy curve of section at 0.5 m behind the pile

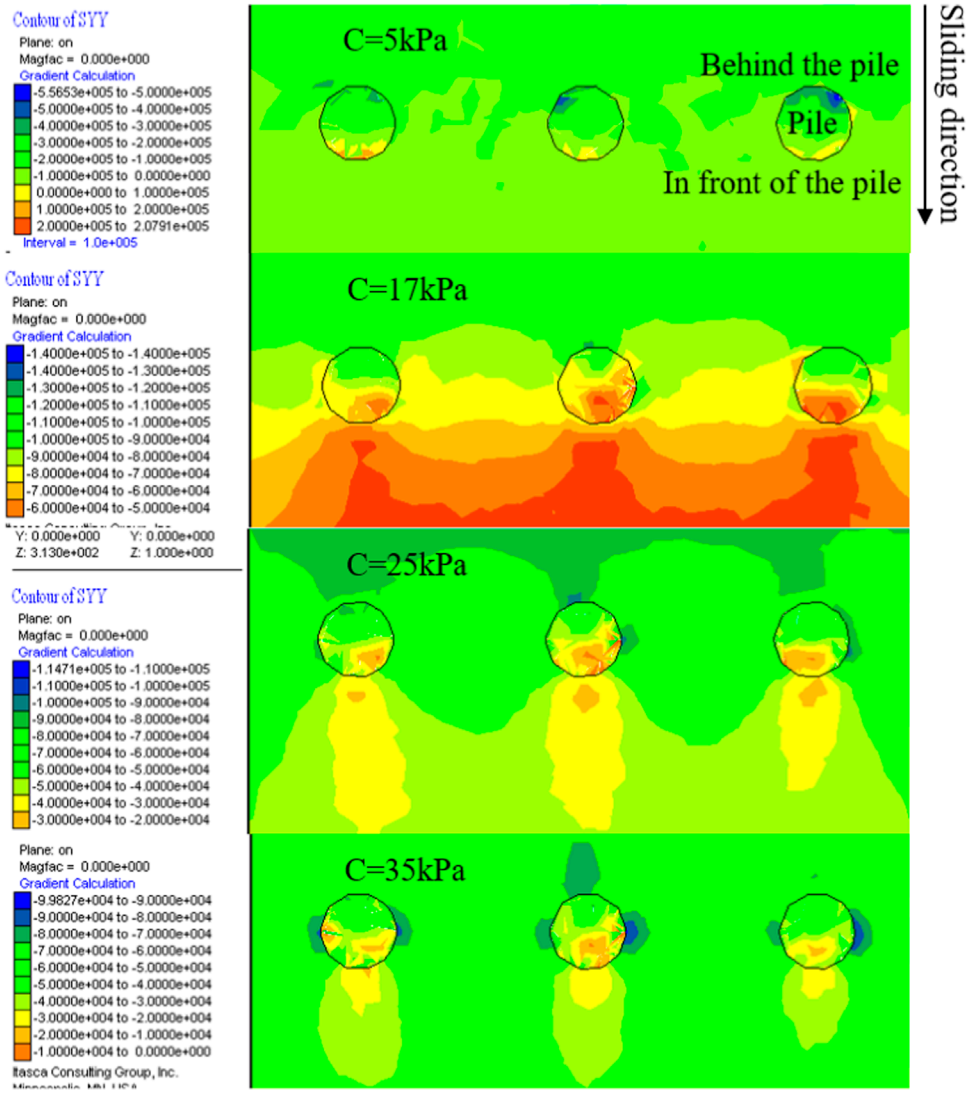


FIGURE 14
The distribution of σy under different cohesions.

becomes smaller, indicating that the anti-sliding effect is enhanced. The stress concentration zone on the anti-slide pile is gradually transferred from the back to the side of the pile. This is because when the value of φ is small, it is mainly the soil arching behind the pile. In contrast, it is mainly the soil arching between piles when the value of φ is high.

The σy curve on the central axis between piles is shown in Figure 18. From the variation range of the curve, it

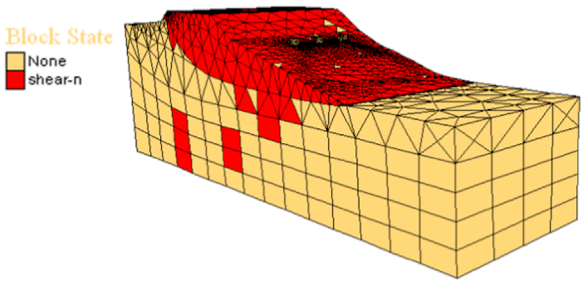


FIGURE 15
The plastic zone at C = 5 kPa.

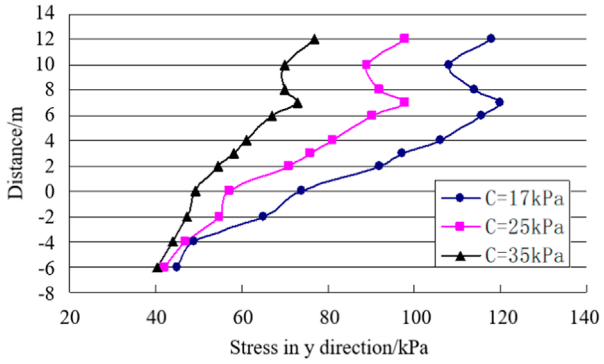


FIGURE 16
The σy curve on the central axis between piles.

can be found that the soil arch effect is the most obvious when φ=10° and the stress in front of the pile have little different in three cases. It shows that when the internal friction angle is 10 o, due to the full play of the soil arch effect, it can play a better anti-sliding effect. This indicates that when the internal friction angle is 10°, the soil arch effect can be fully exerted and the anti-sliding effect can be achieved. The stress is less sensitive to the change of internal friction angle from 17° to 25°. It is shown that the soil arch effect will not be fully effective when the angle of internal friction exceeds 17°.

The σy curve on the central axis in front of the pile is shown in Figure 19. From the stress curve, it can be seen that the σy in front of the pile has a significant change when the internal friction angle increases from 3° to 10°, and the load sharing ratio of the pile is increased by 20%. When the internal friction angle increases from 17° to 25°, the increase of the internal friction angle has little effect on σy, and the pile load sharing ratio is only slightly improved. It is also shown that the soil arch effect will not be fully effective when the angle of internal friction exceeds 17°.

## 3.5 Analysis of the influence of pile spacing on soil arching

Keeping the other parameters of the model unchanged, the influence of the soil arch effect is analyzed by changing the size of pile spacing. S represents the pile spacing, and d represents the pile diameter, three cases of s/d = 2, s/d = 3, and s/d = 5 are set for calculation. The σy nephogram of the cross-section in three cases is shown in Figure 20. It can be seen that with the increase of pile spacing, the soil arch behind the pile becomes gradually gentle, and the soil arch before the pile becomes gradually prominent. When s/d = 5, the soil arching stress in front of the pile is significantly higher than in the other two cases, indicating that extrusion of soil between piles is more pronounced with increased pile spacing.

The σy curve on the central axis between piles in three cases is shown in Figure 21. With the increase of pile spacing, the slope of the curve of the soil arch segment gradually decreases, indicating that the soil arch effect is weakening. The σy in front of the pile gradually increases, indicating that the increase in the pile spacing will lead to a decrease in the anti-sliding effect. When the pile spacing is small, the soil arch effect is obvious, and the landslide thrust is mostly borne by the pile. In comparison, the soil in front of the pile bears more and more load when the pile spacing is large. When the slip resistance in front of the pile is not enough to resist the downward thrust, the anti-slip pile will fail to work. If the pile spacing is too small, the anti-slide pile will be destroyed by over-bearing the sliding stress of the soil behind the pile. While if the pile spacing is too large, the anti-slide stress behind the pile cannot be effectively borne. Therefore, pile spacing is a key factor that should be considered in the design of anti-slide piles.

## 3.6 Analysis of the influence of expansive force on soil arching

The landeslide mass in the area where the landslide is located has certain expansibility, according to which the influence of expansive force on soil arch effect is analyzed, which can provide some basis for the design of anti-slide pile in swelling soil landslides area. In order to simulate the expansive force of soil, the normal stress in x, y, and z directions is applied to each element of soil in FLAC3D. The expansive force is set to 0 kPa, 30 kPa, 60 kPa, 90 kPa and 120 kPa for calculation. According to Figure 22, there is an obvious soil arch effect when there is no expansive force and the expansive force is 30 kPa. When there is no expansive force, the soil arch height behind the pile is higher, and there is a stress concentration area behind the pile, indicating that the stress of soil is transferred to the pile body by the soil arch effect. When the expansive force is 30 kPa, the soil arch at the center line of the pile has been concave, and the stress of the soil in front of the pile has also increased significantly, indicating that the soil arch effect has been weakened. The stress distribution under the three conditions of expansive force of 60 kPa, 90 kPa, and 120 kPa is relatively close. Soil arch cannot be formed between piles and behind piles, and a narrow high-stress area appears in front of piles, indicating that the anti-slide piles have lost the blocking effect on the soil between piles.

The σy curve in front of the pile is shown in Figure 23. When the expansive force changes in the range of 0–60 kPa, the σy before the pile increases significantly with the increase of the expansive force, and the pile load sharing ratio also decreases by 18%. Continuing to increase the expansive force, there was no obvious change in the pile load sharing ratio as the slope was already sheared and damaged.

In order to analyze the sensitivity of shear strength parameters and expansive force to pile-soil effect, the curves of pile load

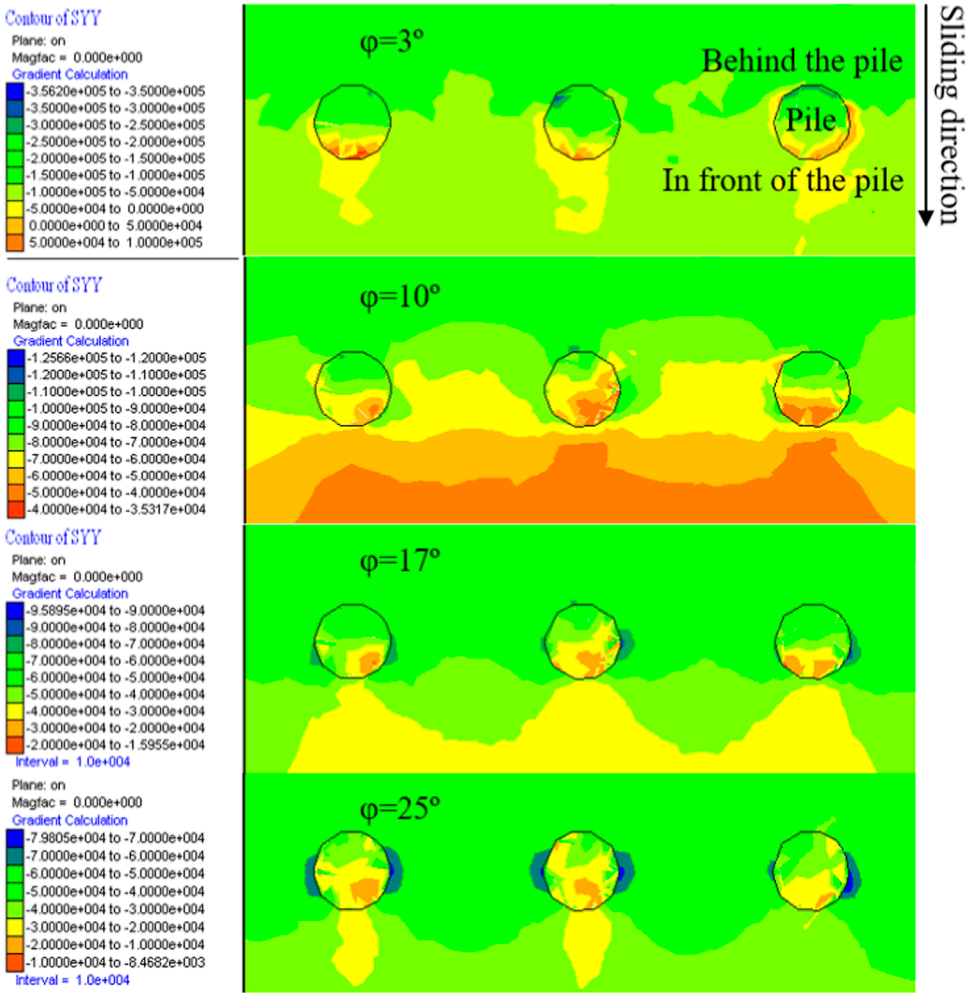


FIGURE 17
The nephogram of σy at different internal friction angles.

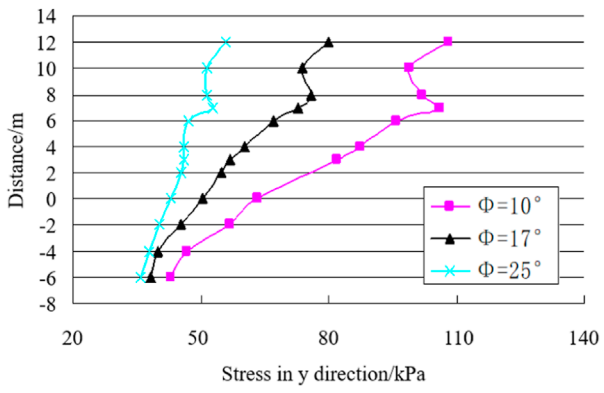


FIGURE 18
The σy curve on the central axis between piles.

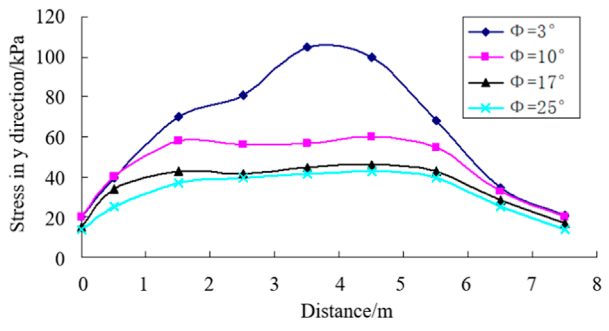


FIGURE 19
The σy curve on the central axis in front of the pile.

sharing ratio with expansive force under different shear strengths are calculated. According to Figure 24, with the increase of shear strength, the load-sharing ratio of the pile increases, and with the increase of expansive force, the load-sharing ratio of the pile decreases. When the expansive force is greater than 60 kPa, it has little effect on the pile load-sharing ratio. In comparison, the influence on the load-sharing ratio of the pile increases with the

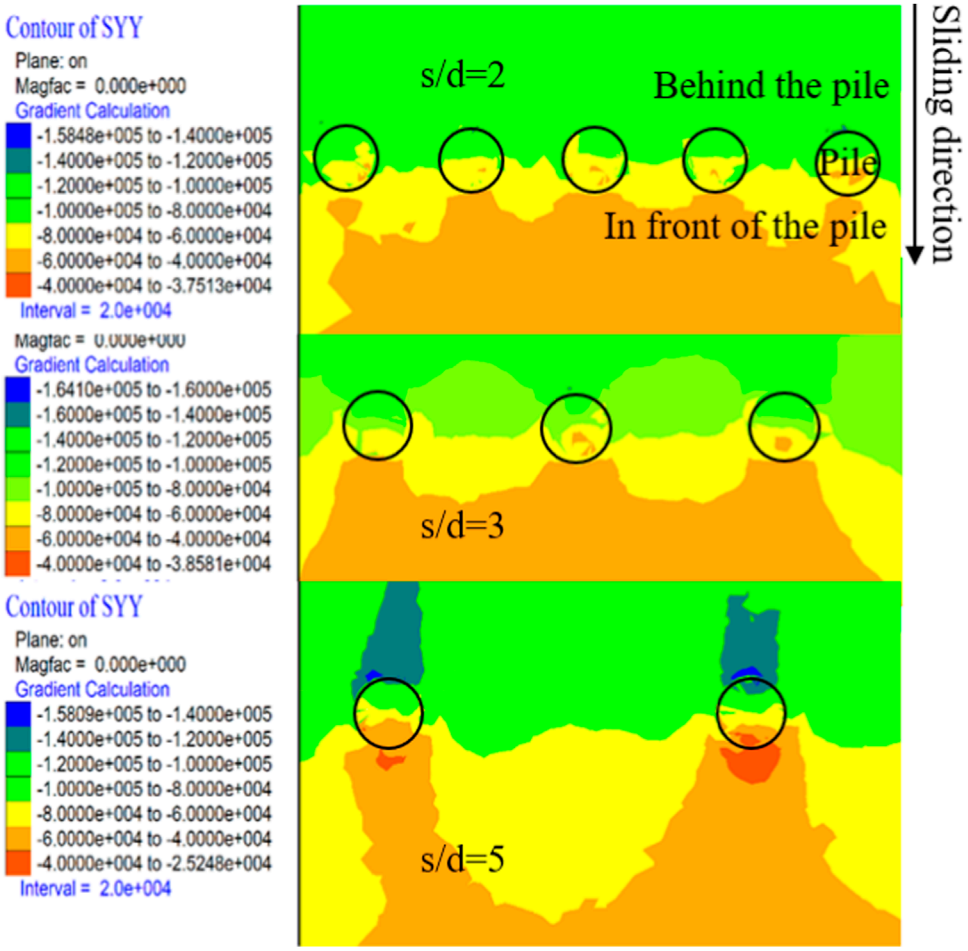


FIGURE 20
The nephogram of σy in different pile spacing.

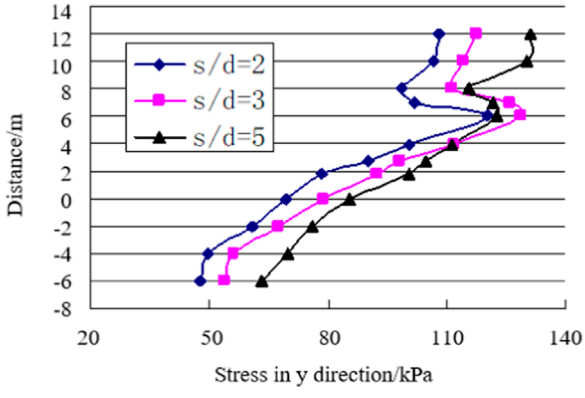


FIGURE 21
The σy curve on the central axis between piles.

decrease of the shear strength parameters when the expansive force is less than 60 kPa. Thus, it can be seen that in the swelling soil landslides area with low shear strength, the existence of expansive force has a certain influence on the anti-slide effect of anti-slide piles, which should be absolutely considered in practical engineering.

## 4 Discussions and conclusions

The formation of soil arch is a kind of "wedge tightening" effect between soil particles. The soil arch generated by the anti-slide pile and the surrounding soil under the action of the residual sliding thrust has the effect of dispersing the sliding thrust, and transmits the force to the anti-slide pile. Most or all of the sliding thrust of the landslide body is mainly shared by the side friction resistance of the anti-slide pile. When the pile side friction is greater than or equal to the sliding thrust of the slope, the soil arch between the piles is formed and the landslide also stops sliding. At the same time, the soil mass between piles should have enough strength to resist the compression deformation generated during the landslide sliding process, so as to have the conditions for the formation of soil arch between piles.

As an objective manifestation of pile-soil interaction, the soil arching effect reflects the effect of anti-slide piles on slope reinforcement from the side. The prerequisite for soil arching is uneven or relative displacement, resulting in a "wedge tightening" effect. Soil arching effect directly affects the anti-slide effect of anti-slide piles. Pile spacing is an important factor affecting soil arching effect, and pile spacing is also a key content of anti-slide pile design. In practical engineering, the determination of pile spacing mainly

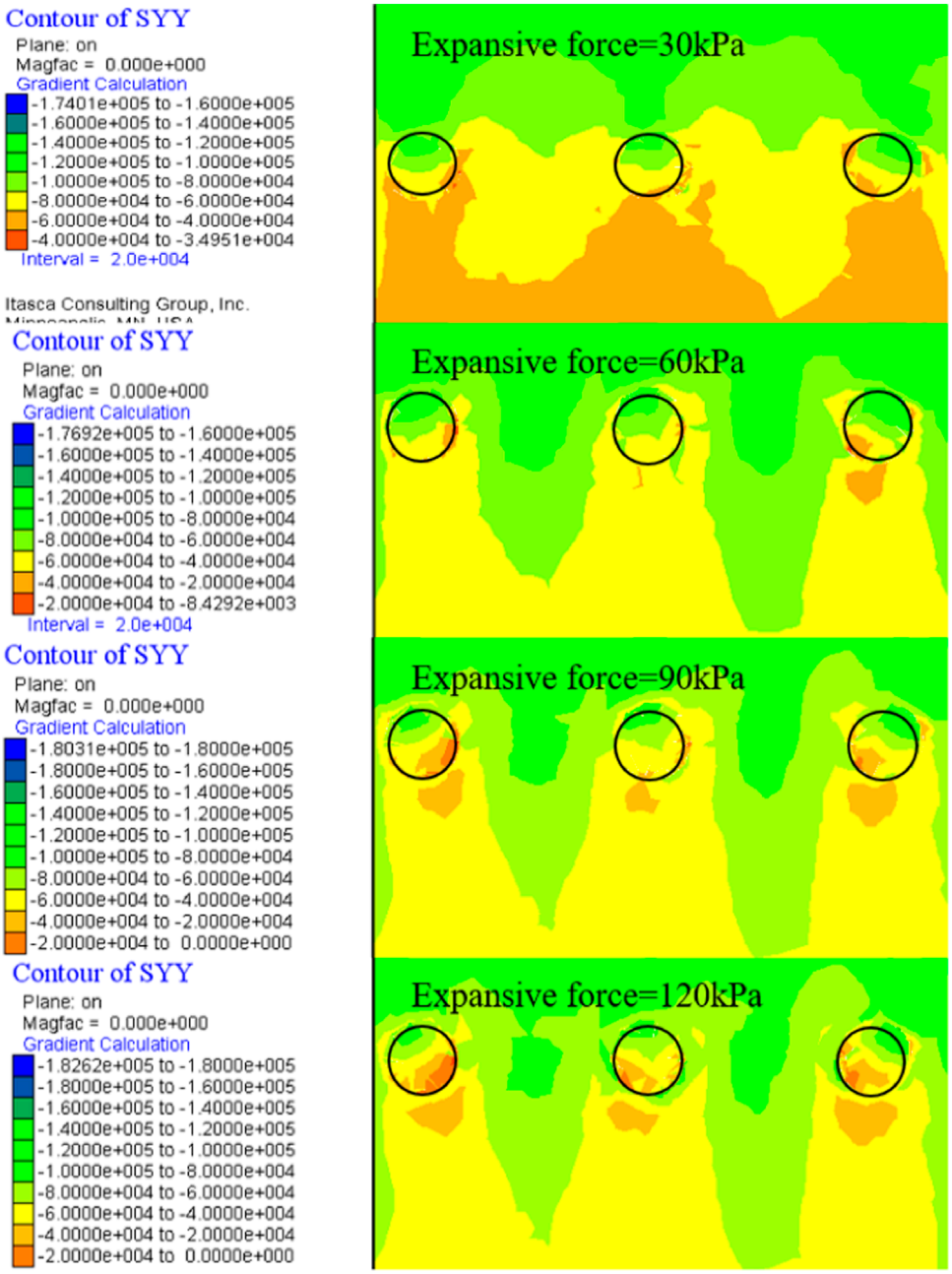


FIGURE 22
The nephogram of σy in different expansive forces.

considers that the friction resistance between the soil and the side of the pile is not less than the landslide thrust between the piles, ignoring the soil arching effect. If the pile spacing is too small, the cost will be too high. If the pile spacing is too large, the soil between piles may slide out from the pile, resulting in slope instability. At the same time, the soil arching effect cannot be produced, and the ability of anti-slide piles to share the sliding thrust of soil becomes worse. Reasonable pile spacing should make the slope have sufficient stability, and the soil between piles will not be squeezed out from the pile under the action of landslide thrust. The cohesion and internal friction angle not only affect the stability of the slope, but also have an important influence on the soil arching effect. The increase of cohesion and internal friction angle will enhance the shear strength of the soil, so as to improve the ' wedge ' effect of the soil between piles, thus enhancing the soil arching effect. The roughness of the pile-soil interface also has a certain influence on the formation of soil arching. In practical engineering, the contact interface between the pile and the soil is certainly rough. During the construction of cast-in-place piles, the soil within a certain range around the pile will also be cemented and solidified under the action of concrete. These factors are not considered in the whole design and calculation process of anti-slide piles. In fact, there is a certain safety reserve

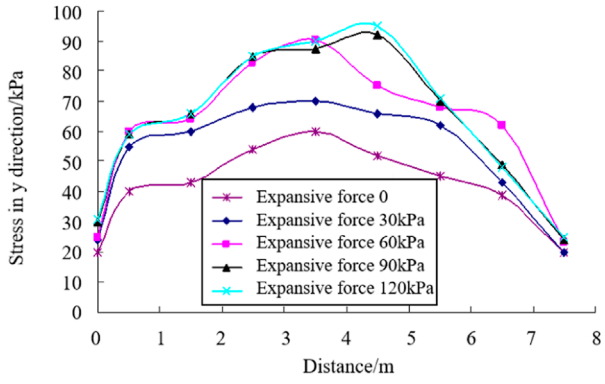


FIGURE 23
The σy curve in front of the pile.

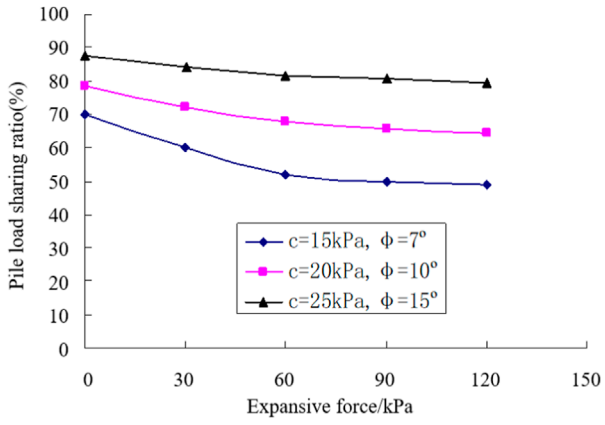


FIGURE 24
The pile load sharing ratio.

of anti-slide force. The sliding thrust of the landslide has a certain influence on the soil arching effect, but it has little effect. After the soil arching is formed, increasing the sliding thrust can only make the soil arches compact each other. When the thrust increases to the critical state, the slope will be unstable and damaged.

Based on the field investigation of geological conditions and genetic mechanism of swelling soil landslides, the formation mechanism and influencing factors of the soil arch effect are studied. The main conclusions are as follows.

(1) The soil arch effect works within a certain depth range. The soil arch effect increases with the increase of depth. In the middle and lower part of the sliding body where the anti-slide pile is located, the soil arch effect reaches the maximum and then gradually weakens. At the position where the soil arch effect is the strongest, the passive side of the pile will produce a tensile stress zone, and the active side will produce stress concentration, which is caused by the soil arch effect transferring the soil stress between piles to the pile body.

(2) According to the curve based on the σy of each point on the central axis between piles, the formation area of the soil arch effect and the change of action strength can be seen intuitively. The load sharing ratio of pile is the key index to reflect the anti-slide effect of anti-slide pile. And the strength of soil arching effect can be analyzed through this index. In addition, the degree of soil settlement can be predicted and analyzed according to the stress curve on the central axis of the anti-slide pile.

(3) The larger the cohesion and internal friction angle, the stronger the soil arch effect, but it only has a greater influence on the soil arching when its value is small. Therefore, attention should be paid to the weakening effect of soil arch effect in soil with low shear strength. Pile spacing has a great influence on the pile load sharing ratio, and the increase of pile spacing will reduce the pile load sharing ratio. The pile spacing is considered an important factor in practical engineering. The expansive force has a great influence on the soil arch effect in the process of the expansive force from scratch. The expansive force also has a great influence on the formation of soil arches for soil with low shear strength. Therefore, in the swelling soil landslides area, the design of anti-slide piles should consider the adverse effects of expansive force.

## Data availability statement

The datasets presented in this study can be found in online repositories. The names of the repository/repositories and accession number(s) can be found in the article/supplementary material.

## Author contributions

PX: Conceptualization, Writing–original draft, Writing–review and editing. XX: Writing–original draft. CJ: Conceptualization, Writing–review and editing. RW: Writing–original draft. JZ: Writing–original draft. XZ: Writing–original draft, Writing–review and editing.

## Funding

The author(s) declare that financial support was received for the research, authorship, and/or publication of this article. This work is sponsored by Research Program of Guizhou Province-ZK (2022) General 166.

## Conflict of interest

Authors PX and CJ were employed by Liaoning Non-Ferrous Geological Exploration and Research Institute Co., Ltd. Author RW was employed by Shenyang Geotechnical Investigation & Surveying Research Institute Co., Ltd.

The remaining authors declare that the research was conducted in the absence of any commercial or financial relationships that could be construed as a potential conflict of interest.

## Publisher's note



## References

Dai, Z. J., Huang, K., Chi, Z. C., and Chen, S. X. (2024). Model test study on the deformation and stability of rainfall-induced expansive soil slope with weak interlayer. *Bull. Eng. Geol. Environ.* 83 (3), 76. doi:10.1007/s10064-024-03576-2

Deng, Y. S., Li, L., Peng, C., Li, L., Liu, J., and Fu, Y. (2022). Model tests on geogrid reinforced pile supported embankment under static and dynamic loads. *Rock Soil Mech.* 43 (8), 2149–2156. doi:10.16285/j.rsm.2021.1829

Deng, Y. S., Li, W. J., Feng, Z. J., Zhang, K. Q., Li, L., Yao, Z. G., et al. (2024). Bearing Characteristics and influence parameters of rigid pile-semi-rigid pile-geogrid reinforced subgrade. *China J. Highw. Transp.*, 37(02), 209–218. doi:10.19721/j.cnki.1001-7372.2024.02.017

Ding, X., He, H., Qu, Y. L., and Yang, Y. X. (2022). Analysis of the pile-soil combined effect of micropiles in strengthening expansive soil landslide in southern shaanxi based on the dynamic soil arch model. *Adv. Mater. Sci. Eng.* 2022, 1–6. doi:10.1155/2022/8114708

Fang, J. J., Yang, X. L., and Feng, Y. X. (2023). Deformation and strength characteristics of expansive soils after suction loading and unloading. *Chin. J. Rock Mech. Eng.*, 42(S2), 4271–4279. doi:10.13722/j.cnki.jrme.2022.0591

Fang, J. J., Yang, X. L., Feng, Y. X., Gong, J., and Niu, H. C. (2021). True triaxial experimental study on mechanical properties of expansive soils after drying and wetting cycles. *Chin. J. Rock Mech. Eng.* 40 (05), 1043–1055. doi:10.13722/j.cnki.jrme.2020.0902

Han, M. Z. (2021). Research on pile-soil interaction effect in soft soil foundation. *Dalian Univ. Technol.* doi:10.26991/d.cnki.gdllu.2020.000120

Hu, P. (2022). Optimization of anti slide pile based on soil arching effect. *Chongqing Jiaot. Univ.* doi:10.27671/d.cnki.gcjtc.2021.000446

Hu, X. L., Liu, D. Z., Niu, L. F., Liu, C., Wang, X., and Fu, R. (2021). Development of soil-pile interactions and failure mechanisms in a pile-reinforced landslide. *Eng. Geol.* 294, 106389. doi:10.1016/j.enggeo.2021.106389

Huang, Y., Xu, L., Zhou, J., and Cai, Y. (2020). Calculation of pile-soil stress in pile-net composite foundation based on improved Terzarghi method. *Rock Soil Mech.* 41 (2), 667–675. doi:10.16285/j.rsm.2019.0050

Li, X., Yan, E. C., Tian, Z., and Zhang, Y. (2021). Stress-reduction model for soil arch and its application in load sharing model for landslide. *J. Northeast. Univ. Nat. Sci.* 42 (3), 436–443. doi:10.12068/j.issn.1005-3026.2021.03.020

Li, X. S., Li, Q. H., Wang, Y. M., Liu, W., Hou, D., Zheng, W. B., et al. (2023). Experimental study on instability mechanism and critical intensity of rainfall of high-steep rock slopes under unsaturated conditions. *Int. J. Min. Sci. Technol.* 33 (10), 1243–1260. doi:10.1016/j.ijmst.2023.07.009

Liu, B., Wang, X. M., Liu, C. H., and Kong, J. C. (2023). Effect of relative stiffness of pile and soil on pile group effect. *J. Mar. Sci. Eng.* 11 (1), 192. doi:10.3390/jmse11010192

Liu, Z. Z., Yan, Z. X., Wang, X. G., Li, J. W., and Qiu, Z. H. (2021). Effect of the inclined pile-soil arch in a soil landslide reinforced with anti-sliding piles. *Nat. Hazards* 106 (3), 2227–2249. doi:10.1007/s11069-021-04541-y

Ren, X., Hu, Y., Wang, R., Bai, L., and Ma, J. (2022). Formation mechanism of passive soil archin front of embedded section of anti-slide piles. *Chin. J. Undergr. Space Eng.* 18 (2), 642–649. doi:10.3969/j.issn.1673-0836.2022.2.dxkj202202034

Sun, S. W., Ma, N., Hu, J. B., and Zhu, B. Z. (2019). Evolution characteristics and mechanism analysis of soil arch of anti-slide pile. *J. Railw. Eng. Soc.* 36 (11), 7–12. doi:10.3969/j.issn.1006-2106.2019.11.002

Tan, B., Pan, Z. A., Xu, L., and Wang, J. (2024). Laboratory investigation of lateral swelling pressure of nanning grey-white expansive soil. *Soil Mech. Found. Eng.* 60 (6), 521–527. doi:10.1007/s11204-024-09924-4

Tian, Y. L., Qiu, Y. F., Xian, L., and Liang, J. H. (2021). Mechanism of swelling rock and soil landslides and key technologies for treatment. *Fresenius Environ. Bull.* 30 (4), 3622–3631.

Wang, G., Li, C., He, X., Zhang, Y., Yao, W., Song, C., et al. (2022). Physical model test on the effect of different anchoring methods on the mechanical and deformation characteristics of anchored slide-resistant piles. *Bull. Geol. Sci. Technol.* 41 (6), 262. doi:10.19509/j.cnki.dzkq.2022.0151

Wang, K. Y., Ye, J. H., Wang, X. Q., and Qiu, Z. L. (2024). The soil-arching effect in pile-supported embankments, A review. *Buildings* 14 (1), 126. doi:10.3390/buildings14010126

Wang, M. (2022). Influence of different pile spacing on soil arching effect of single row cantilever anti-slide piles. *Eng. J. Wuhan Univ.* 55 (S1), 49–53.

Wang, T., Zhang, L., Liao, F., Wang, J., Lan, X., Xu, T., et al. (2023). Analysis of anti-slide performance of slide-resistant piles of aviation fuel pipeline under landslide disaster. *J. Disaster Prev. Mitig. Eng.* 43 (2), 250. doi:10.13409/j.cnki.jdpme.20211101001

Xu, L., Zhang, L., and Gong, H. (2021). Near-Fault seismic response of large-span CFST tied arch bridge considering soil-pile interaction. *J. Chongqing Jiaot. Univ. Nat. Sci.* 40 (10), 63–72. doi:10.3969/j.issn.1674-0696.2021.10.08

Xu, Y. (2020). Hydraulic mechanism and swelling deformation theory of expansive soils. *Chin. J. Geotechnical Eng.* 42 (11), 1979–1987. doi:10.11779/CJGE202011002

Yang, G., Chen, Z., Zhang, H., Duan, J., Xia, X., and Lin, Y. (2022). Collapse mechanism of gentle expansive soil slope in drying and wetting cycles. *J. Central South Univ. Sci. Technol.* 53 (1), 95–103. doi:10.11817/j.issn.1672-7207.2022.01.005

Zhang, Q., Jia, C. J., Chen, H. J., Zheng, Y. N., and Cheng, W. (2024). Centrifuge modeling test on reactivation of ancient landslide under sudden drop of reservoir water and rainfall. *Acta Geotech.* doi:10.1007/s11440-023-02217-4

Zhang, R., Zhao, X., Zheng, J., and Liu, Z. (2020). Experimental study and application of lateral swelling stress of expansive soil. *China J. Highw. Transp.* 33 (9), 22–31. doi:10.19721/j.cnki.1001-7372.2020.09.003

Zhang, S. F., Li, C., Qi, H., Chen, X. J., and Ma, S. S. (2021). Soil arch evolution characteristics and parametric analysis of slope anchored anti-slide pile. *Ksce J. Civ. Eng.* 25 (11), 4121–4132. doi:10.1007/s12205-021-1612-6

Zhang, Y., She, X., and Gao, X. (2018). Experimental study on mechanical characteristics of Lijiaping tunnel expansive surrounding soils and analysis of tunnel collapse. *J. Water Resour. Water Eng.* 29 (1), 203–208. doi:10.11705/j.issn.1672-643X.2018.01.35

Zhang, Z., Lin, Y., He, H., Zhang, H., and Yang, G. (2022). Instability characteristics and stability analysis of expansive soil slope. *J. Central South Univ. Sci. Technol.* 53 (1), 104–113. doi:10.11817/j.issn.1672-7207.2022.01.006

Zhu, C., He, M. C., Karakus, M., Cui, X. B., and Tao, Z. G. (2020). Investigating toppling failure mechanism of anti-dip layered slope due to excavation by physical modelling. *Rock Mech. Rock Eng.* 53 (11), 5029–5050. doi:10.1007/s00603-020-02207-y